





Article

Toward Synthetic Data Generation to Enhance Skidding Detection in Winter Conditions

Bryan McKenzie * , Souso Kelouwani  and Marc-André Gaudreau 

Département de Génie Mécanique, Université du Québec à Trois-Rivières, Trois-Rivières, QC G8Z 4M3, Canada
* Correspondence: bryan.mckenzie@uqtr.ca

Abstract: In this paper, we propose the use of a neural network to identify lateral skidding events of road vehicles used during winter driving conditions. Firstly, data from a simulation model was used to identify the essential vehicle dynamics variables needed and to create the network structure. Then this network was retrained to classify real-world vehicle skidding events. The final network consists of a 3 layer network with 10, 5 and 1 output neurons 13 inputs, 4 outputs and a 5 step time delay. The retrained network was used on a limited set of real vehicle data and confirmed the effectiveness of the network classifying lateral skidding events.

Keywords: side-slip; winter driving; artificial neural network



Citation: McKenzie, B.; Kelouwani, K.; Gaudreau, M.-A. Toward Synthetic Data Generation to Enhance Skidding Detection in Winter Conditions. *World Electr. Veh. J.* **2022**, *13*, 231. <https://doi.org/10.3390/wevj13120231>

Academic Editors: Wuhong Wang and Lisheng Jin

Received: 15 October 2022

Accepted: 23 November 2022

Published: 2 December 2022

Publisher's Note: MDPI stays neutral with regard to jurisdictional claims in published maps and institutional affiliations.



Copyright: © 2022 by the authors. Licensee MDPI, Basel, Switzerland. This article is an open access article distributed under the terms and conditions of the Creative Commons Attribution (CC BY) license (<https://creativecommons.org/licenses/by/4.0/>).

1. Introduction

Increasing car safety is an ongoing concern for all manufacturers. During the last few decades, several electromechanical systems have increased overall car safety. These devices include anti-lock braking, electronic stability control and lane departure warning systems among others. Most of these systems, however, have limitations. Firstly, these systems were designed for use with a human driver as part of the vehicle system. The presence of a human in the control loop greatly reduces the need for vehicle control as the systems are only there to assist the drivers in certain very specific situations and rely on the driver when these systems underperform [1–5]. Secondly, none of these systems take into consideration that the tire-road force generation may be fluctuating or can be very low. This situation happens quite often in several different driving conditions, including cold winter conditions. This situation can lead to large undesirable vehicle path deviations on snowy or icy roads making it difficult for the driver to correct the vehicle dynamics and avoid an incident [1–5]. Thirdly, these systems have been developed for internal combustion engines and their specific dynamics. As all types of electric vehicles become more prominent, it has become clear that these systems do not allow for an optimal use of the electric drive's faster reaction capabilities both from a safety and an energy efficiency standpoint. It is therefore necessary to design new control systems with the targeted vehicle type and class to ensure proper optimization.

It is essential to have a very good estimate of the tire-road interaction to be able to properly calculate the effects of the proposed change to the vehicle steering wheel angle or the acceleration and brake torque. Without the ability to estimate possible skidding of the wheels with regards to the road surface, it is impossible to finely control vehicle dynamics [6]. This information can take many forms, tire side-slip and slip-ratio estimations, tire force estimations, tire-road friction coefficient estimation or simply an indication of impending skidding. Only with this information can the control system take appropriate decisions. With this knowledge we can conclude that the current state of autonomous vehicle development and currently used mass-market technology does not allow complete vehicle autonomy (SAE International levels 4–5 autonomy levels) for all driving conditions [5–9].

Tire dynamics are quite complex, non-linear and vary over time due to tire tread wear and vehicle loading. Winter driving conditions are mostly unexplored and are particularly complex as the tire-road reaction effort is a function of numerous factors. The temperature, tire type, tire wear, vehicle loading, the presence of snow and/or ice and the use of road abrasives and salts affect the ability of a tire to transmit efforts to the roadway [7,10–12]. This situation is further complexified by the fact that the tire can be exposed to different road conditions over a short amount of time. Most classical model driven approaches fail in predicting and classifying wheel and vehicle dynamics accurately in real time. The use of GNSS navigation data is promising [6] but is still limited as signal availability is not guaranteed and resolution may vary to a degree that it becomes irrelevant for vehicle dynamics calculations. Compensation using different varieties of optimal estimation, Kalman filters or sliding mode observers, are promising but performance degrades as GNSS signal unavailability increases because of acceleration integration drift [6,10–12]. The currently available sensor system in cars does not allow precise calculation of wheel slip parameters and full dynamic knowledge of the wheel states and requires the addition of sensors to the vehicle [13,14].

Over the last two decades, several studies have explored the use of artificial intelligence as a means of overcoming the complexity of using classical vehicle dynamic models [15–21]. Many of the studies conclude that the highly nonlinear nature of a complete vehicle coupled with the varying nature of the different parameters make the classical models inefficient when used for real-world vehicle control. Neural networks can be structured and trained to represent these non-linear behaviours, even if the entire model is not known, if given the appropriate input and training data. As can be observed from several sources. The use of simulation data from high-fidelity simulators can generate data that can be used to train the neural networks to adjust their weights and biases to properly predict the looked-for vehicle dynamics or behaviour [18–21]. It must be understood by the creator of such a neural network that the predictive performance of such a tool now resides on the network structure and on the quality and quantity of the data that is used to train the network [22]. As only a certain aspect of the vehicle dynamics is usually looked for, in the case of most of these studies; either the side-slip angle or the friction coefficient, the neural network can therefore forego several data inputs that do not influence the output being estimated, something that is very difficult to do using classical vehicle models as the model hypotheses usually require all the selected inputs to be present [18].

In their article, Fang et al. [18] focuses on the creation of a neural network that is initially trained using simulation data as it is easily generated. The network was then used with real world data obtained from a highly instrumental vehicle. Tests were run on dry and wet asphalt to vary the road friction coefficient resulting in a low error when estimating the vehicle acceleration and angular acceleration with regards to the vertical axis. This methodology was used for many articles reviewed. As for most of the available literature, no tests were run on real road conditions in winter driving situations [1]. Although using a different variant, X. Lu, X. Zhang, G. Zhang et al. [19], develop a functional neural network for the control of an omnidirectional vehicle using four separate motors for propulsion and direction. Aalizadeh in the article [23], compared a neurofuzzy algorithm and a standard 3 layer 20-10-1 neural network for the identification of yaw rate, for three different driving manoeuvre and two different road surface coefficients. The article demonstrates a standard neural network is very accurate at estimating the yaw rate given a limited number of vehicle dynamics information.

The current study has two goals; firstly, identifying what is the minimum vehicle dynamic parameters that must be used to properly identify wheel side-slip and secondly identifying all lateral skidding events that have occurred with high accuracy while being driven in real winter conditions. All vehicle dynamics information currently available on the vehicle CAN-bus is considered available for the current study. Wheel mounted sensors have been added to the vehicle wheels to be able to capture the y-axis acceleration (ISO 8855-2011 axis definition). Skidding is defined as the moment that the lateral or longitudinal

tire reaction force no longer increase even though the vehicle steering or propulsion systems indicate that the reactions should increase (inability of the tire-road interaction to increase the reaction efforts). Classification error close to 0 is assumed to be necessary considering that the safety of the occupants and bystanders are at risk.

In the proposed method, the first step is to simulate realistic vehicle dynamics data (including wheel y-axis acceleration) using CarSim™ software and use the information to prepare a preliminary artificial neural network (ANN) able to predict wheel lateral (side-slip) slip. For the first step, it is hypothesized that a network's ability to identify the correct tire side-slips will allow a future network to correctly classify real world skid events. The simulation data will be obtained using CarSim™ software. As real world vehicle testing consumes large amounts of time can put drivers in dangerous situations and generates data that requires a high amount of work to process adequately, the first step is to correctly identify what variables are required to set up an optimized ANN using simulated data. The second step will use the proven network structure and minimum data input, obtained from the first step, to create a new ANN that is able to classify the tire behaviour as "skidding" or "not skidding" from real world vehicle tests done during winter driving conditions in a controlled setting. The results of the first and second part of this study will be used to fully equip a test vehicle with dynamic sensors and run extensive tests in all types of driving conditions, both in a simulation and the real world, and fully optimize the detection algorithm for use in a generalized setting (all types of driving weather and conditions).

The major contributions of this work are as follows:

- (1) Identifying the minimal vehicle dynamic information requirements needed to identify real world slipping,
- (2) Creating an ANN able to classify the skidding with high accuracy.

2. Materials and Methods

2.1. Vehicle Models Commonly Used

Modelling a complete vehicle is a complex task. The number of parts, the highly non-linear behaviours of several components and the lack of appropriate models to represent some components are some of the reasons modelling vehicles has proven to be such a challenge. Additionally, vehicle parameters change drastically over time due to several factors including component wear, material property variability, vehicle loading, road surface conditions and so on. Several different sources use several different simplified models to predict vehicle dynamics. Among the most popular are the bicycle model, see Figure 1 and the 4-wheel model, see Figure 2. Equations (1)–(8) describe these models [6,24,25]. As can be seen from these models they do not take into consideration the tire dynamics or the tire-road interaction, these are assumed to be infinitely rigid and having no slip. These models are not very useful in determining wheel slip as they do not model the tire-road interactions.

Vehicle centre of gravity (CoG) bicycle model ignoring road bank angle is given by Equation (1).

$$ma_y = F_{yf} + F_{yr} \quad (1)$$

where m , a_y , F_{yf} and F_{yr} are the vehicle mass, centre of mass y-axis acceleration, front tire lateral force and rear tire lateral force, respectively. The lateral acceleration is defined as:

$$a_y = \dot{y} + V_x \dot{\psi} \quad (2)$$

where \dot{y} , V_x and $\dot{\psi}$ are vehicle lateral acceleration due to pure lateral tire motion, vehicle centre of mass x-axis velocity and z-axis angular velocity (yaw rate). Substituting (2) into (1) we obtain 3.

$$m(\dot{y} + V_x \dot{\psi}) = F_{yf} + F_{yr} \quad (3)$$

To add the lateral tire forces to the system of equations the underlying small side slip hypothesis must be understood. These equations do not consider low friction road surfaces. The tire-road interaction is summed up in the cornering stiffness coefficient, $C_{\alpha f}$ [24].

$$F_{yf} = 2C_{\alpha f}(\alpha_f) \quad (4)$$

$$F_{yr} = 2C_{\alpha r}(-\alpha_r) \quad (5)$$

where $C_{\alpha f}$ and $C_{\alpha r}$ are the tire proportionality constants and α_f and α_r are the angles between the tire orientation and the direction of travel. The angles between the direction of the tire and their paths can be calculated using the small angle approximations as (6) and (7), respectively, [24].

$$\alpha_f = \frac{\dot{y} + a\dot{\psi}}{V_x} \quad (6)$$

$$\alpha_r = \frac{\dot{y} - b\dot{\psi}}{V_x} \quad (7)$$

where \dot{y} is the vehicle y-axis velocity. Finally, the model needs the moment balance about the z - axis to be complete.

$$I_z\ddot{\psi} = aF_{yf} - bF_{yr} \quad (8)$$

where a and b are the distances between the vehicle centre of mass and front and back wheel centre of masses. Finally, I_z and $\ddot{\psi}$ are the vehicle z-axis inertia and vehicle z-axis angular acceleration.

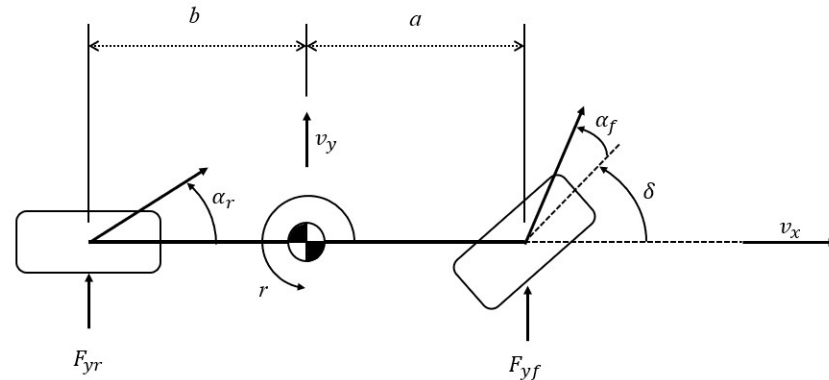


Figure 1. Typical vehicle bicycle model [6,8,13,24,26,27].

The simple four-wheel vehicle model in Figure 2 follows almost identical dynamic equations modelling but with the addition of the two missing wheels. The limitations remain the same, no proper tire-road interaction and very simplified tire models.

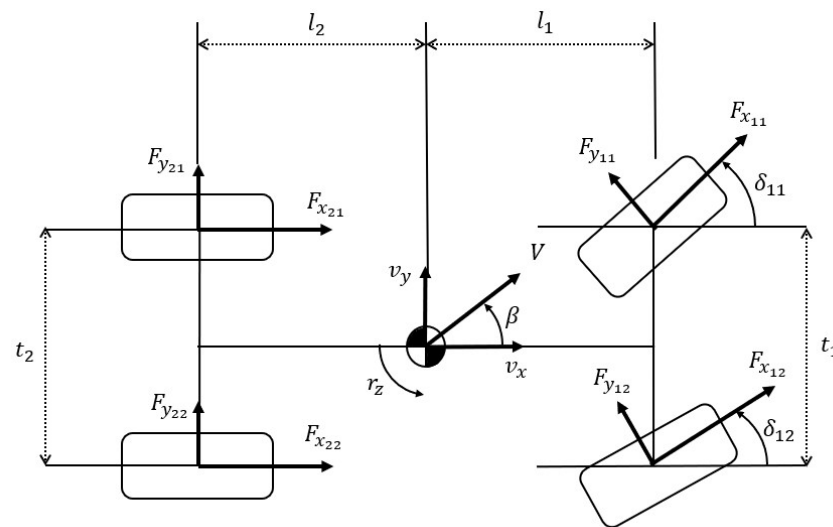


Figure 2. Typical simplified vehicle model [6,8,13,24,26,27].

Tire modelling is very complex and not completely understood [26]. Several different tire models have been developed in the last 100 years. Among the most advanced, accurate and used models are the Magic Formula series of models. These are all semi-empirical models and require several parameters and scaling factors to produce accurate results [26]. For an in-depth analysis of the formulas, parameters and scaling factors please refer to chapter 4 of [26]. The parameters and scaling factors are; tire construction, tire stiffness, inflation pressure, load, temperature, wear and rotation speed, requiring the model to be updated at every calculation step to produce adequate results over a long period. Although work is ongoing on smart tires [28], the technology has yet to be deployed to the mass market. Therefore, the use of tire models are of limited help in actually determining side slip as they also suffer from the same limitations as the previously described models, they are computationally heavy, need to be updated as conditions change and current sensors do not produce the required data for real-time parameter update.

To get a good understanding of longitudinal and lateral tire maximum reaction forces, Figures 3 and 4 depict the slip versus force of a tire when modelled using the *MFSWIFT* formula [27,29–35]. The *MFSWIFT* tire model is a computationally simplified tire model based on the complete magic formula tire model. It is extensively used for simulation purposes because of its accurate representation of tire dynamics and very quick calculation time. One of this paper's hypotheses is that the final classification network is able to detect skidding based on the fact that a similar network was good at estimating side slip (or slip ratio) [36,37]. The fact that tires exhibit quasi-linear behaviour when the slips are small and then exhibit non-linear behaviour before saturating indicates that the final artificial neural network (ANN) should be able to classify the change given some sort of time history allowing the network to recognize the change from the quasi-linear region to the non-linear region [38–40]. As to keep implementation costs low, this should be done using only currently available car sensor data along with the addition of wheel lateral acceleration. Although this paper's objectives deal exclusively with lateral tire slip, it is fully understood that tires have a traction limit that is a function of both the longitudinal and lateral tire dynamics [41–44].

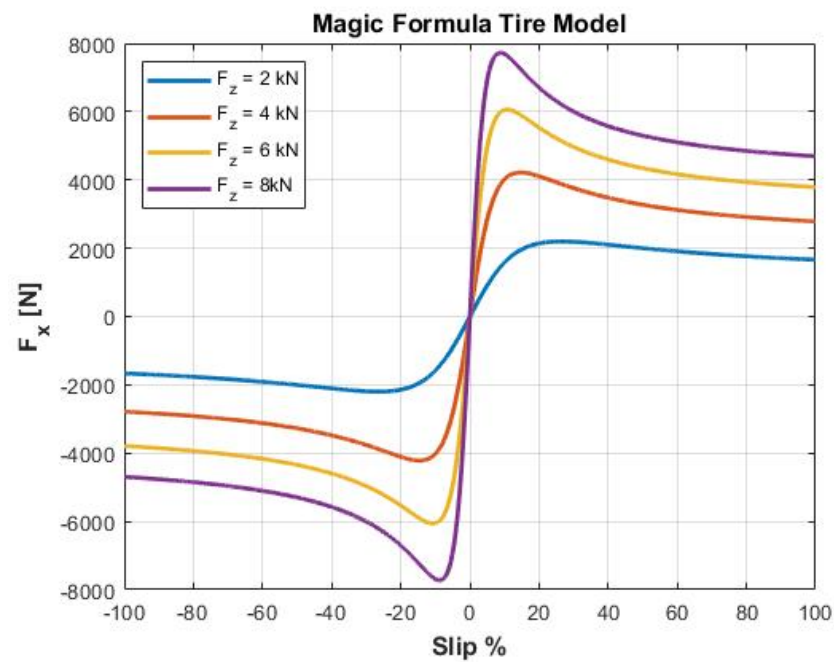


Figure 3. Generic tire longitudinal slip ratio vs. longitudinal force for different normal tire force cases.

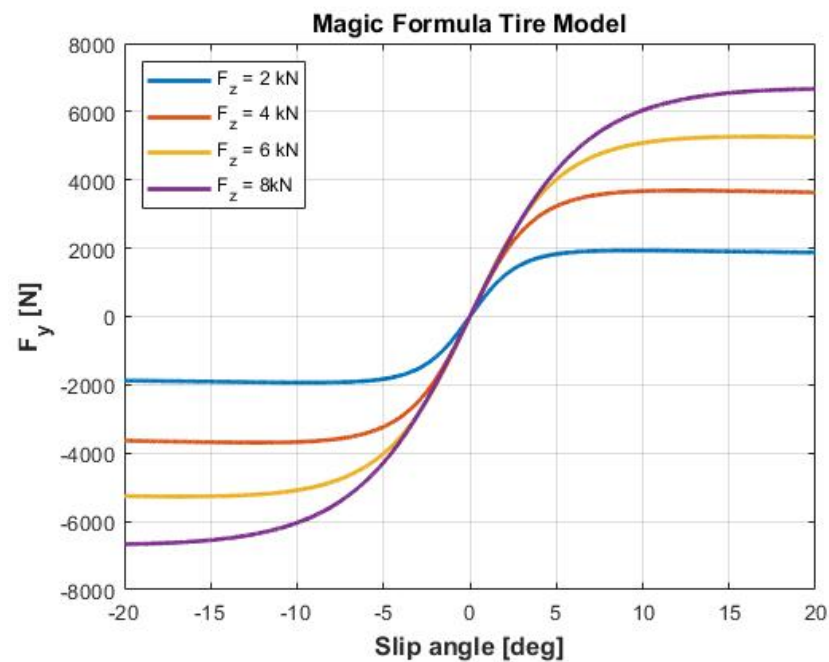


Figure 4. Generic tire lateral side slip angle vs. lateral force for different normal tire force cases.

Published studies have used different variants of the Kalman filter (most used side slip optimal state estimator) to fusion data and obtain the tire slip angle [13,34,45,46]. The Kalman filter is a linear estimator and slip angle dynamics are non-linear with a high dimensional making this state estimator valid for only short periods of time while the non-linear response can be estimated by a linear model. Since most classical method tries to approximate this non-linearity, they will provide a rough side-slip estimation which makes it difficult to further perform a good skidding classification.

Although this technique gives good results, most studies use a global navigation satellite signal (GNSS) as the necessary measurement to add to the update step of the Kalman filter estimator. Although it is possible for the Kalman filter [47] to also use the

wheel lateral acceleration as the necessary input to estimate the wheel side-slip, the limited capacity to adequately model the vehicle will usually lead to the use of artificial intelligence to fill in the model gaps, therefore it is deemed more efficient to use the ANN to directly compute the side slip or skid events.

Several commercially available highly complex vehicle simulation systems are available. Among these are CarsimTM, AutoSim ASTM, ADAMSCarTM and The MathworksTM Simscape-Vehicle-Template-21.1.2.6. These systems model most vehicle parts and interactions and are able to produce vehicle data that is of high enough quality to use as design and optimization tools. These systems, however, require enormous computational resources to produce these results. Energy, space and weight available on road vehicles do not allow these types of systems to be currently used for real-time on-board computing. Additionally, given the safety concerns with relying on an enormously complex software system to provide real-time critical information for assisting in safety-critical decision-making, a functional safety assessment and testing will be required and would add several software and hardware layers for redundancy, increasing the size and computational requirements even further [48]. Therefore, these types of systems are not well suited for on-board applications.

The inherent complexity, changing conditions and limited computational resources available to indicate the use of an artificial neural network as valid tool for the estimation of side-slip and the classification of vehicle skidding [15–17]. The neural network, when adequate inputs, structure and training are used, are able to develop high levels of non-linear relationships even when the system dynamics are not well understood. Vehicle dynamics are causal but are not fully understood or modelled accurately, therefore time-delayed-neural network has the required structure to create the required links between several input variables and the target output. Analysis of the different vehicle models, tire models and side slip equations [24], indicates that there is always at least one parameter missing from most vehicle on-board sensors. Be it, wheel load [24], tire deformation [28], lateral tire force [7] or self-aligning moment reduction [24] are missing to accurately estimate tire lateral slip in all driving conditions. For this article $\alpha_{wheel,y}$ has been selected as the additional piece of information. Wheel y-axis acceleration can very easily be obtained through a micro-electro-mechanical sensor (MEMS) which are readily available and cost effective. In this study, wireless sensors were placed directly on the wheel hub as this requires minimal investment and yields direct results for wheel y-axis acceleration. The sensor could also be placed on any portion of the vehicle's suspension that is stiffly connected to the wheel in the wheel y-axis (i.e., steering knuckle) to be able to connect the sensor through a wired connection.

2.2. Neural Network Structures

Two different types of neural networks will be used, one for the side slip estimation and a second for the classification of skid events.

The first neural network will be regressive and is used to estimate the side slip angle of a each wheel. Firstly, it will be trained using simulation data and create a baseline network for the next network [49]. The second network will be a discriminating network that will classify real-world vehicle dynamics into a “skidding” and “not skidding.”

The side-slip estimation uses a supervised time-delayed feed-forward regression neural network (TDNN) that outputs a value that can range from $-\infty$ to ∞ . Although the output could be composed of continuous values from $-\infty$ to ∞ , the side slip angle rarely exceeds 20 degrees [0.4 rad] as tire lateral skidding often occurs at this point. Although not presented in this report, substantial work was done using a nonlinear autoregressive network with exogenous inputs (NARX) and nonlinear autoregressive network (NAR) types. Training yielded good results, $R > 0.9$, but failed to report good results when using validation and testing data. The cause of the bad results is the use of the previously estimated side slip as an input value for the network. This leads the network to diverge quite rapidly.

The need to have high resolution output values without being subjected to asymptotic maximum or minimum value behaviour indicates that the final activation function should be a linear output activation function. The outputs of other hidden layers should also be able to vary in the negative and positive values to allow the directional nature of the values being calculated to filter through the network during training. The tangent-sigmoid activation function will be used for these layers.

The network was trained using the Levenberg–Marquardt training algorithm. This training algorithm is commonly used for a large variety of different neural network training given its versatility [50–53]. The Levenberg–Marquardt training algorithm was successfully used to train a 3 layer 10-8-1 standard neural network for the identification of rubber-ice friction coefficient in a laboratory setting in Gao et al.’s study [50]. Although in different fields of interest, this training algorithm is very successful for the standard and time-delayed neural network as is mentioned in [52,53].

Several different neural network training algorithms were also tested to ensure that it was the optimal solution for this problem. The highly non-linear nature of the problem indicates that the scaled conjugate gradient should be a quick option for this task. The scaled conjugate gradient training algorithm was close to 100 times faster than the Levenberg–Marquardt algorithm but with a decrease in the regression factor of one half. This low regression factor is insufficient for the task being done and the scaled conjugate gradient algorithm was not used. The same pattern, although not as pronounced, was observed for several different training algorithms including; resilient back propagation, Fletcher-Powell conjugate gradient and one step secant. The behaviour of the vehicle is highly causal as demonstrated above, and the network will have increased accuracy by having time delayed elements. The amount of time delayed inputs will have to be adjusted for the final real-world data as the acquisition frequency will dictate the amount needed.

The final network size was obtained by the optimization of the network using the list of linearly important variables, see Table 1 for the list used. A series of different network structures were created where the number of neurons per layer varied. The optimization required several training, testing and validation cycles be run for several different first and second layer neuron quantities. The results (MSE) of each combination was plotted and compared to the others. The simplest network that showed high levels of performance (small MSE) was used to keep the final network as small as possible. The network selected was a 3 layer network, with 10, 5 and 1 neurons for each layer, respectively. Adding extra neurons or layers did not increase the network’s ability estimate side-slip with a significantly lower performance error. See Figure 5 for iteration values, all testing was done using 17 input variables.

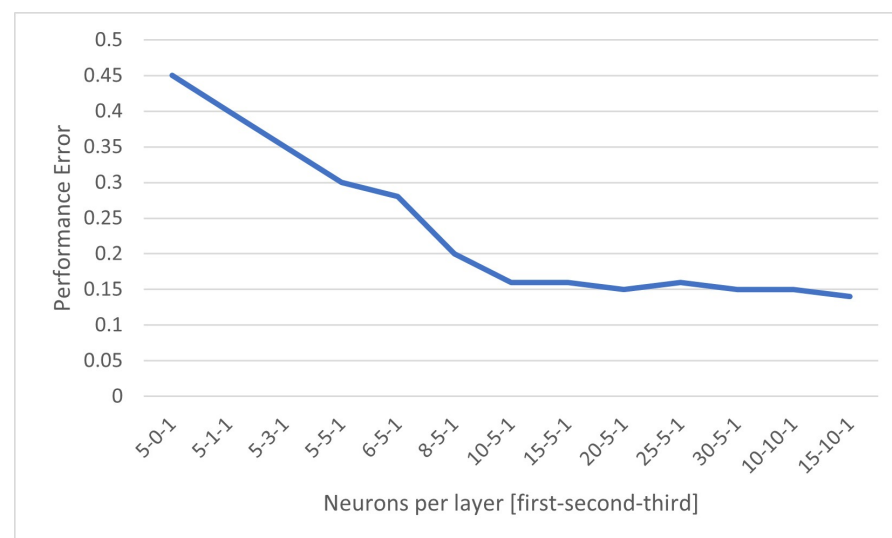


Figure 5. Performance error versus network size with 13 final variables.

The tire-road interaction is the limiting factor in transferring lateral road reactions. With this definition, the problem at hand can be easily be formulated in terms of probability rules. Equation (9) demonstrates this in the form of Bayes' rule.

$$P(\text{SideSlip} | Y(f, \text{input})) = \frac{P(Y(f, \text{input}) | \text{SideSlip})P(\text{SideSlip})}{P(Y(f, \text{input}))} \quad (9)$$

The second network will have the same structure but will be discriminative given that the goal is not to estimate but rather to classify, more information is presented in Section 3.2.

3. Results

3.1. Simulated Vehicle Dynamics

In the context of this study, an optimized ANN will be one that has minimized the number of inputs while maintaining a low error and be sufficiently computationally light to be able to output values at a frequency greater than 60 Hz.

Data was generated from several different vehicle configurations and steering maneuvers (8 electric vehicle configurations and 18 different routes including different road friction coefficients, where μ is equal to 1, 0.6 or 0.3).

As the original data obtained from the simulation models is free of any noise or perturbations, it is important to test the proposed ANN architecture with data containing noise. This will ensure that the network is adequately stable and generalized before starting work on real-world data. The data obtained from the simulation was modified by adding white Gaussian noise (MATLAB™R2021b function "awgn" with a SNR of 30 dB, leading to approximately 5% SNR). The signal was then filtered using a sliding average filter with 25 sample size window using the MATLAB™R2021b function "slidingavg".

As the simulation model outputs several hundred variables, it is essential to select the variables that are the most efficient at estimating the desired output, wheel side-slip angles, while reducing the number of input variables. A three-level feature selection process was used to reduce the amount of input variables to a minimum. The first filter was to remove all variables that are not available, either directly or through direct calculation, on the test car either through the vehicle CAN bus or through the addition sensors available. The second variable reduction was made through the use of linear and non-linear feature selection [22]. The last filter was a correlation study to ensure that the input variables do not exhibit high levels of correlation as those that do must be excluded as to not induce a system bias with regards to the correlated data [22].

The vehicle dynamics parameters that are available on the test car are included in Table 2. This list became the starting point for the second step of the input variable selection. Global navigation satellite system (GNSS) data was removed as signal availability is not guaranteed. The use of optimal state estimators can compensate the slow update speed and possible lack of signal for a certain time, this technology cannot as of yet be relied upon for real-time side-slip estimation. The even though the data was not going to be used, it was nonetheless left in the two feature selection steps to verify the significance of these elements.

Two different feature selection tools were used. The first linear (input to target) filter type feature selection tool, the minimum redundancy maximum relevance algorithm was used. For this study the MATLAB™R2021b "fsrmmr" function was used. This tool was selected as not only does it maximizes the linear relevance between the input and the target but it also minimizes the redundancy of the input variables. This tool is extremely useful as the removal of input data that has exhibited correlation must be removed. The result of this filtering is shown in Table 1. The remaining variables were considered not significant due to their low-linear relationship.

Table 1. Sorted list of linearly related input variables.

Rank	Dynamics Variable	Description	Unit
1–4	$a_{y_{wheel_i}}$	Wheel y-axis Acceleration	[m/s ²]
5	a_z	Vehicle Acceleration z-axis	[m/s ²]
6	v_x	Vehicle Velocity x-axis	[m/s]
7	θ_{sw}	Steering Wheel angle	[-]
8	a_y	Vehicle Acceleration y-axis	[m/s ²]
9	$\dot{\omega}_x$	Vehicle Angular Accelerations x-axis	[s ⁻²]
10	ω_y	Vehicle Angular Velocities y-axis	[s ⁻¹]
11	ω_z	Vehicle Angular Velocities z-axis	[s ⁻¹]
12	$\dot{\omega}_z$	Vehicle Angular Accelerations z-axis	[s ⁻²]
13	$\dot{\omega}_y$	Vehicle Angular Accelerations y-axis	[s ⁻²]
14	\dot{a}_{wheel_y}	Wheel y-axis Jerk	[m/s ³]
15	a_x	Vehicle Acceleration x-axis	[m/s ²]
16	\dot{a}_y	Vehicle Jerk y-axis	[m/s ³]
17	ω_x	Vehicle Angular Velocity x-axis	[s ⁻¹]

Table 2. List of potential network input variables.

Dynamics Variable	Description	Unit
θ_{sw}	Steering Wheel angle	[-]
τ_{MT}	Motor Load	[%]
v_x	Vehicle Velocity x-axis	[m/s]
a_i	Vehicle Acceleration	[m/s ²]
\dot{a}_i	Vehicle Jerk	[m/s ³]
ω_i	Vehicle Angular Velocities	[s ⁻¹]
$\dot{\omega}_i$	Vehicle Angular Accelerations	[s ⁻²]
$\ddot{\omega}_i$	Vehicle Angular Jerk	[s ⁻³]
ω_{wheel}	Wheel Angular Velocity	[s ⁻¹]
v_{wheel_y}	Wheel Velocity (calculated using effective radius)	[m/s]
$a_{y_{wheel_i}}$	Wheel y-axis Acceleration	[m/s ²]
$\dot{a}_{y_{wheel_i}}$	Wheel y-axis Jerk	[m/s ³]

This first type of filter does not verify if there are any non-linear relationships between the inputs and the target. Therefore a sequential wrapper feature selection tool was used. For this study the MATLAB™R2021b “sequentialfs” function was used. This algorithm selects subsets from the original list that result in the lowest error and does so until there are no longer any improvements. As with all wrapper methods used in feature selection, this feature selection tool needs to run the full ANN training using the different subsets to compare the results. To do this efficiently a three layer (10, 5 and 1 neurons per layer) feed-forward neural network was used. This step clearly identified that the angular acceleration in the vehicle *x-axis*, $\dot{\omega}_x$, was extremely important. The remaining variables were an order of magnitude less significant. The sorted results are presented in Table 3.

A correlation (Pearson correlation with a *p*-value 0.05 significance level) was run to reduce the risk that the non-independent data be over-represented in the network’s output. When the 12 input signals (including the lateral acceleration of each wheel) resulting from

first filtering steps were run for correlation, it is clear that many of the variables exhibit large correlation. The major contributor of this situation stems from the nature of the data used. Most of the data is that of the vehicle rolling in a relatively straight line with very few lateral events, therefore leading the data concerned with lateral dynamics to be very similar for large portions of the time. If the final network is to be generalized for most driving scenarios, the inclusion realistic driving scenarios must be maintained. This indicates that the network will have to function properly regardless of the presence of data exhibiting linear correlation. Correlation heat map is shown in Figure 6 (This might lead to the need to have side-slip range specific ANN being used to help alleviate the linear correlation issue as to separate the data with low lateral dynamics from the data with higher lateral dynamics.)

Table 3. Sorted list of variable following wrapper methods

Rank	Dynamics Variable	Description	Unit
1	$\dot{\omega}_x$	Vehicle Angular Accelerations x-axis	[s ⁻²]
2–5	$a_{y_{wheel_i}}$	Wheel y-axis Acceleration	[m/s ²]
6	v_x	Vehicle Velocity x-axis	[m/s]
7	θ_{sw}	Steering Wheel angle	[-]
8	a_y	Vehicle Acceleration y-axis	[m/s ²]
9	a_z	Vehicle Acceleration z-axis	[m/s ²]
10	ω_y	Vehicle Angular Velocities y-axis	[s ⁻¹]
11	ω_z	Vehicle Angular Velocities z-axis	[s ⁻¹]
12	$\dot{\omega}_z$	Vehicle Angular Accelerations z-axis	[s ⁻²]
13	$\dot{\omega}_y$	Vehicle Angular Accelerations y-axis	[s ⁻²]
14	ω_x	Vehicle Angular Velocity x-axis	[s ⁻¹]
15	a_x	Vehicle Acceleration x-axis	[m/s ²]
16	\dot{a}_{wheel_y}	Wheel y-axis Jerk	[m/s ³]
17	\dot{a}_y	Vehicle Jerk y-axis	[m/s ³]

A variable probability density analysis was also run for each variable. By far most variables exhibit Gaussian distribution with a very narrow spread and centred around 0. A few variables, including vehicle and wheel y-axis acceleration, have a bimodal behaviour where most data is focused around the mean but significant number of samples are observed close to the variable maximums and minimums. This behaviour is quite consequential to the observed vehicle paths. They represent the saturation values before vehicle skidding occurs. This is highly useful information as it indicates that these variables should be good indicators of vehicle skidding.

The TDNN uses 13 input variables and 4 output variables that can be found in Table 4. As the system is causal, adding several time delays, 5 in the case of this study, to the input structure is an efficient way a transferring the causality to the network outcome. The network structure diagram is shown in Figure 7. This network functions using the 13 input variables at $t_0, t_{-1}, t_{-2}, t_{-3}, t_{-4}$ for a total of 65 total inputs. All the most important input combinations have been tested to ensure that the final input variables were optimal. The results are presented in Figure 8.

Table 4. Final list of input variables.

Rank	Dynamics Variable	Description	Unit
1–4	$a_{y_{wheel_i}}$	Wheel y-axis Acceleration	[m/s ²]
5	a_z	Vehicle Acceleration z-axis	[m/s ²]
6	v_x	Vehicle Velocity x-axis	[m/s]
7	θ_{sw}	Steering Wheel angle	[-]
8	a_y	Vehicle Acceleration y-axis	[m/s ²]
9	$\dot{\omega}_x$	Vehicle Angular Accelerations x-axis	[s ⁻²]
10	ω_y	Vehicle Angular Velocities y-axis	[s ⁻¹]
11	ω_z	Vehicle Angular Velocities z-axis	[s ⁻¹]
12	$\dot{\omega}_z$	Vehicle Angular Accelerations z-axis	[s ⁻²]
13	$\dot{\omega}_y$	Vehicle Angular Accelerations y-axis	[s ⁻²]

3.2. Real Vehicle Dynamics

Understanding the real world data flow is important to be able to correctly analyze any sources of data degradation or any time delays in the different data streams. The main issue stemming from the preliminary data collection run is the maximum available frequency that the currently used data collection is able to run. The OBD2-bus recorder used can collect the data at a 10 Hz rate. As will be seen further, this has proven to be adequate for the classification during post treatment but it is likely that this rate is too slow if the information is to be used for vehicle control purposes [48]. The reminder of the data-flow analysis does not indicate any particular issues with the treatment of the data as long as the data can either all be collected at the same time. The data was then filtered using the same filter as with the noised simulated data.

Analysis of the correlation data from the real world testing has revealed a greater amount of signal disparity than the simulation data analysis. This is to be expected given the amount of sensor noise and real world disturbances. The reduced signal correlation will need to be further investigated in a future study with a greater sample size as the disparity in the simulation and the real world data is quite large and only by increasing sample size and sensor data frequency will adequately statistical analysis be valid.

As the side-slip value is unknown using the real world data, the network's key performance index was changed from identifying the slip angle to classifying each time step as skid or no skid. Before setting up further and exhaustive testing, it was essential to prove that the neural network structure was able to classify skidding events on short test runs. Three test runs were conducted on a non-standardized test path running a simple steering direction change on icy conditions on a packed gravel road. Skidding events were identified by the test car driver during testing.

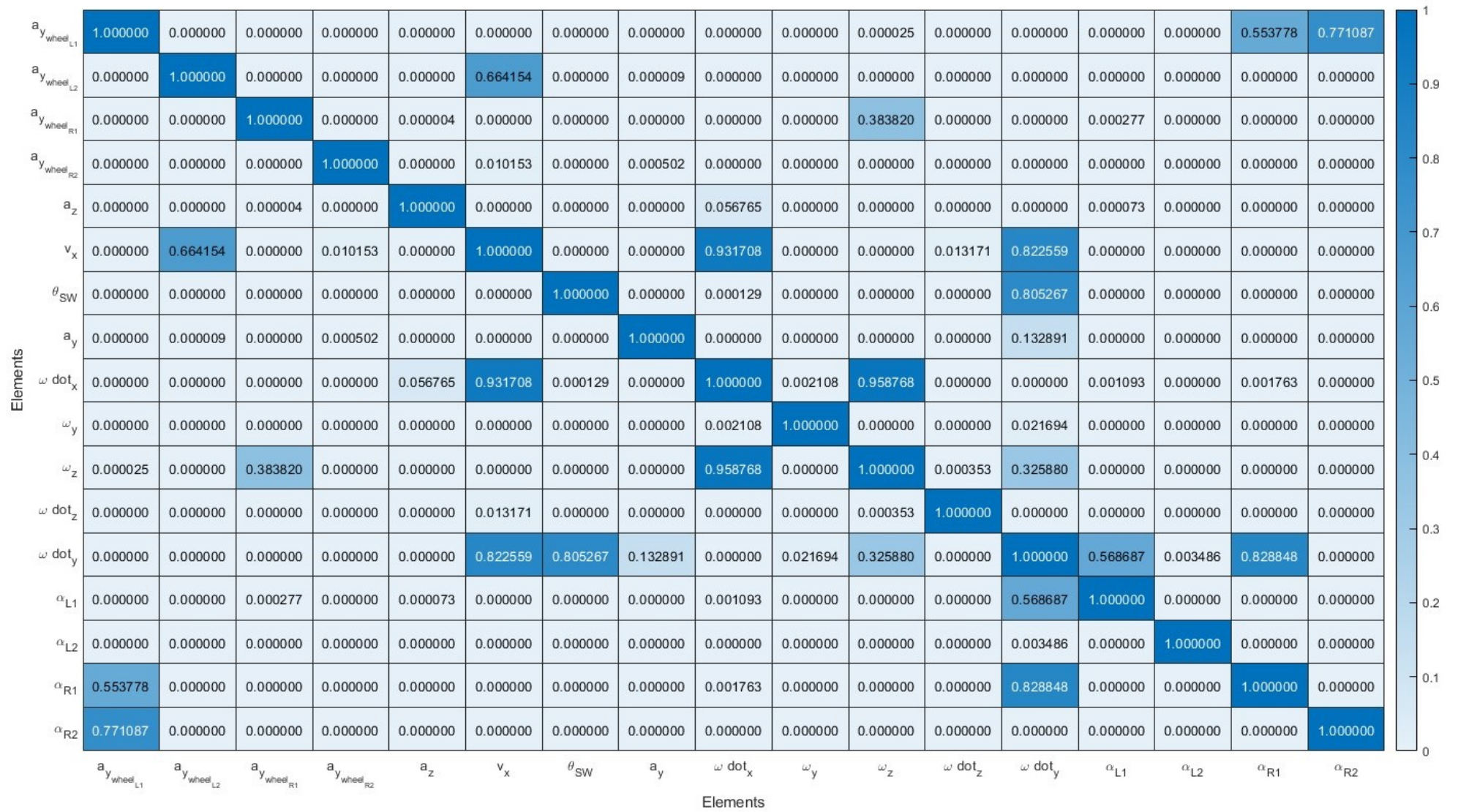


Figure 6. Correlation heatmap of final variables.

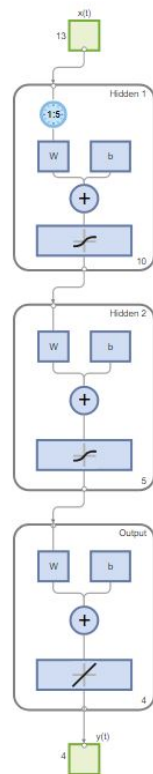


Figure 7. Architecture of final 13-input artificial neural network.

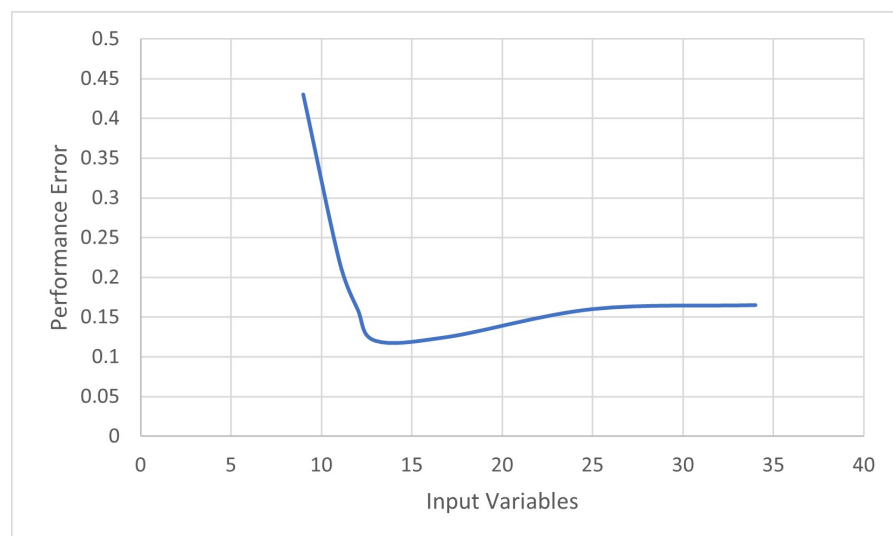


Figure 8. Number of input variables versus performance error with 10-5-1 network structure.

Using the same TDNN as was developed for the previous step, the network was retrained with the real world data and a simple binning layer was added to classify the results. Although it has been shown that the currently used data has been recorded at a frequency that is not adequate for real-time identification, excellent classification will justify further research as the proposed network will be an excellent starting point for the complete implementation. Classification of the skid events was done with 100 % accuracy. Figure 9, shows the results before the binning layer as the results of the binning layer were trivial to show. The last regressive layer before the binning shows that there is quite good regression coefficient indicating network stability. The final network regression (prior to

binning) MES yields a performance coefficient of 4.5126×10^{-6} and a R-value in excess of 0.9999.

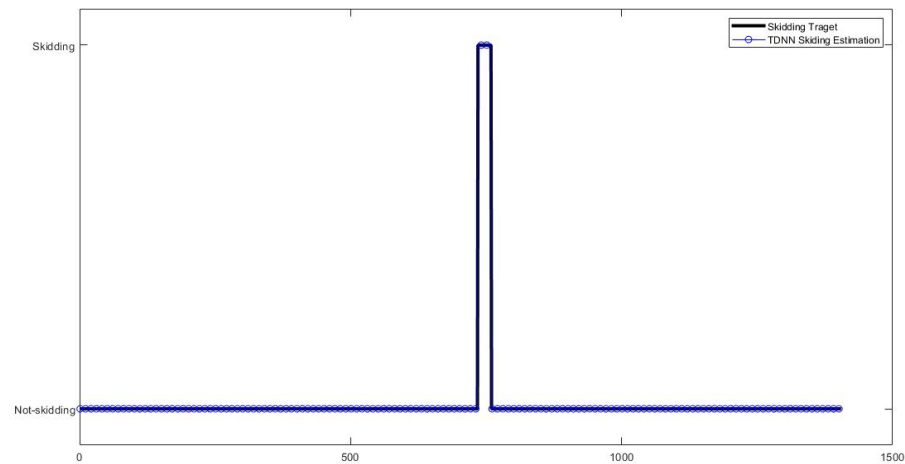


Figure 9. Results of skidding event classification for run 1 of the real world testing.

4. Discussion

The side-slip estimation performance gives satisfactory results when using simulated data. The classification ANN has also correctly classified the skid events of all three real-world tests. This is a strong indication that the proposed network structure can be further generalized using a similar approach but with a much larger real-world data set.

When looking at the final series of input variables and comparing them to the classic full vehicle model, it is interesting to notice that many of the retained variables are the same. Vehicle longitudinal speeds, vehicle lateral and vertical accelerations, steering wheel angle (proportional to wheel angle), and vehicle pitch and yaw rates are all base line pieces of information for the classical models. This information is to be expected as these elements or their integrals which are obtainable by the ANN with the use of the time-delayed elements, have strong linear dependencies with the side-slip calculations. Additionally these variables exhibit a very strong linear correlation with the different wheel side-slip values. The high level of importance of the three components of angular acceleration is an unexpected result. This has mainly been identified during the wrapper method feature selection. As these variables did not rank as high during the minimum redundancy maximum relevance feature selection, it is indicative of a non-linear relationship in the case of a neural network estimation. Additionally, the vehicle angular accelerations are not directly measurable and are therefore not present in the current literature. The vehicle angular accelerations can be very easily calculated for use in an ANN as all the information is readily available as long as a 6-axis inertial unit is available. The optimal time step that needs to be used for the numerical calculation of each derivation will have to be done using real-world data where precise side-slip information is available.

The real world data acquisition that was used for this study was too slow for real time identification of side-slip angles or skidding events and the available sensor hardware needs to be analyzed to ensure that it will be adequate for the intended purpose (battery life and ingress protection are major issues). The network will need to be optimized once better quality data is available from the real world vehicle. These elements should only lead to a better quality network and better estimation.

Lastly, as manual indication of skidding is prone to error, a more robust technique is needed to identify skidding. The vehicle will need to be outfitted with additional sensors to be able to accurately calculate the side-slip angle of the different wheels and identify the exact time when the tire reaction forces change from having a quasi-linear reaction to a

non-linear behaviour that occurs before and during skidding. This will allow the precise calculation of the wheel side-slips and allow mathematical calculations of skidding.

As the results of this research indicates, the addition of wheel-mounted sensors to obtain the y-axis acceleration, combined with the information already available on most production automobiles and the time-delayed neural network developed can lead to excellent estimation of tire side-slip using synthetic winter driving data. The network was also tested using a limited amount of real vehicle data. Again the results were very convincing. This information is crucial in the advance of autonomous vehicles as the controller needs to be able to have this information in order to accurately control a vehicle in all types of weather. This will allow a vehicle controller to apply the optimal correction to ensure the vehicle stays on the desired course.

5. Conclusions

A good understanding of the input and output variables and the relationship between them is needed to correctly create and train an ANN. Several steps were taken to ensure that only the minimum number of inputs were used to generate side-slip estimation with simulated data. After the feature selection phase, 13 inputs were selected as the optimal value for side-slip estimation of the four wheels. This resulted in a network with the ability to estimate the side-slip angle with an average error of 0.04° for each wheel. The network structure was tested using a limited amount of real-world data and showed excellent classification of the skidding events, for three trial runs with driver identified skidding events. Therefore it can be concluded that the two objectives of this paper have been fully realized. The results also warrants further investigation using more extensive standardized vehicle testing.

The real world data acquisition that was used for this study was too slow for real time identification of side-slip angles or skidding events and the available sensor hardware needs to be analyzed to ensure that it will be adequate for the intended purpose. An additional study using normalized real world testing will be run with updated sensors. The network will need to be updated with the better-quality data and then run in real time.

Lastly, as manual indication of skidding is prone to error, a more robust technique is needed to identify skidding. The vehicle will need to be outfitted with additional sensors to be able to accurately calculate the side-slip angle of the different wheels and identify the exact time when the tire reaction forces change from a quasi-linear reaction to the non-linear behaviour that occurs before and during skidding. This will allow the precise calculation of the wheel side-slips and allow mathematical calculation of skidding without the need to include human identification for network training.

Author Contributions: Conceptualization, B.M., S.K. and M.-A.G.; methodology, B.M.; software, B.M.; validation, B.M., S.K. and M.-A.G.; formal analysis, B.M. and S.K.; investigation, B.M.; data curation, B.M.; writing—original draft preparation, B.M.; writing—review and editing, S.K. and M.-A.G.; visualization, B.M.; supervision, S.K. and M.-A.G.; project administration, B.M. All authors have read and agreed to the published version of the manuscript.

Funding: This research has been funded by the Canadian Urban Transit Research & Innovation Consortium (CUTRIC), Natural Sciences and Engineering Research Council of Canada and the Canada Research Chair Program.

Data Availability Statement: Data for this study can be made available through email, send a request to the main author.

Acknowledgments: The author acknowledges the contribution of Muhammad A. Alam, Ali Amamou, Medhedi Oueslati and Alexandre Montambeault for their technical assistance.

Conflicts of Interest: The authors declare no conflict of interest.

Abbreviations

The following abbreviations are used in this manuscript:

ANN	Artificial neural network
CAN	Controller area network
GNSS	Global navigation satellite system
GoG	Center of Gravity
MEMS	Micro-electro-mechanical systems
TDNN	Time-delayed neural network
NAR	nonlinear auto-regressive
NARX	nonlinear auto-regressive network with exogenous inputs
SNR	Signal to noise ration
OBD2	On-board diagnostic 2

References

1. Klouttse Ayevide, F. (Université du Québec à Trois-Rivières, Trois-Rivières, Québec, Canada). Internal Literature Review, 2021.
2. Mohammed, A.S.; Amamou, A.; Ayevide, F.K.; Kelouwani, S.; Agbossou, K.; Zioui, N. The Perception System of Intelligent Ground Vehicles in All Weather Conditions: A Systematic Literature Review. *Sensors* **2020**, *20*, 6532 [CrossRef] [PubMed]
3. D. O. Transport. Weather Impact on Safety. Available online: https://ops.fhwa.dot.gov/weather/q1_roadimpact.htm (accessed on 20 September 2022)
4. NHTSA. Traffic Safety Facts. Available online: <https://crashstats.nhtsa.dot.gov/Api/Public/ViewPublication/812806> (accessed on 20 September 2022)
5. SAE J3016: Levels of Driving Automation. S. International. 2019. Available online: <https://www.sae.org/news/2019/01/sae-updates-j3016-automated-driving-graphic> (accessed on 20 September 2022)
6. Ahn, C.; Peng, H.; Tseng, H.E. Robust Estimation of Road Frictional Coefficient. *IEEE Trans. Control Syst. Technol.* **2013**, *21*, 1–13. [CrossRef]
7. Nam, K. Application of Novel Lateral Tire Force Sensors to Vehicle Parameter Estimation of Electric Vehicles. *Sensors* **2015**, *15*, 385–401. [CrossRef] [PubMed]
8. Nanthakumar, A.J.D.; Baisya, D.; Shrivastava, S. Development of mathematical model for real time estimation and comparison of individual lateral tire force generation. *Mater. Today Proc.* **2021**, *45*, 6755–6766. [CrossRef]
9. Angelo, B.; Andrea, F.S.T.; Nicola, A. Combined regression and classification artificial neural networks for sideslip angle estimation and road condition identification. *Veh. Syst. Dyn.* **2019**, *58*, 1766–1787.
10. Thomaidis, G.; Kotsiourou, C.; Grubb, G.; Lytrivis, P.; Karaseitanidis, G.; Amditis, A. Multi-sensor tracking and lane estimation in highly automated vehicles. *IET Intell. Transp. Syst.* **2013**, *7*, 160–169. [CrossRef]
11. Zang, S.; Ding, M.; Smith, D.; Tyler, P.; Rakotoarivelo, T.; Kaafar, M.A. The Impact of Adverse Weather Conditions on Autonomous Vehicles: How Rain, Snow, Fog, and Hail Affect the Performance of a Self-Driving Car. *IEEE Veh. Technol. Mag.* **2019**, *14*, 103–111 [CrossRef]
12. Lee, U.; Jung, J.; Shin, S.; Jeong, Y.; Park, K.; Shim, D.H.; Kweon, I.S. EureCar turbo: A self-driving car that can handle adverse weather conditions. In Proceedings of the IEEE/RSJ International Conference on Intelligent Robots and Systems (IROS), Daejeon, Korea, 9–14 October 2016; pp. 2301–2306.
13. Novi, T.; Capitani, R.; Annicchiarico, C. An integrated artificial neural network–unscented Kalman filter vehicle sideslip angle estimation based on inertial measurement unit measurements. *Proc. Inst. Mech. Eng. Part J. Automob. Eng.* **2018**, *233*, 1864–1878. [CrossRef]
14. Marti, E.; de Miguel, M.A.; Garcia, F.; Perez, J. A Review of Sensor Technologies for Perception in Automated Driving. *IEEE Intell. Transp. Syst. Mag.* **2019**, *11*, 94–108. [CrossRef]
15. Grip, H.; Imsland, L.; Johansen, T.; Kalkkuhl, J.; Suissa, A. Vehicle sideslip estimation. *IEEE Control. Syst.* **2009**, *29*, 36–52.
16. Hsu, Y.H.J.; Laws, S.M.; Gerdes, J.C. Christian. Estimation of Tire Slip Angle and Friction Limits Using Steering Torque. *IEEE Trans. Control Syst. Technol.* **2010**, *18*, 896–907. [CrossRef]
17. Melzi, S.; Sabbioni, E. On the vehicle sideslip angle estimation through neural networks: Numerical and experimental results. *Mech. Syst. Signal Process.* **2011**, *25*, 2005–2019. [CrossRef]
18. Fang, P.; Cai, Y.; Chen, L.; Wang, H.; Li, Y.; Sotelo, M.A.; Li, Z. A high-performance neural network vehicle dynamics model for trajectory tracking control. *Inst. Mech. Eng. Part D J. Automob. Eng.* **2022**. [CrossRef]
19. Lu, X.; Zhang, X.; Zhang, G.; Fan, J.; Jia, S.. Neural network adaptive sliding mode control for omnidirectional vehicle with uncertainties. *ISA Trans.* **2019**, *86*, 201–214. [CrossRef]
20. Zhang, C.; Wang, C.; Wei, Y.; Wang, J. Neural network adaptive position tracking control of underactuated autonomous surface vehicle. *J. Mech. Sci. Technol* **2020**, *34*, 855–865. [CrossRef]
21. Huang, W.; Wong, P.K.; Wong, K.I.; Vong, C.M.; Zhao, J. Adaptive neural control of vehicle yaw stability with active front steering using an improved random projection neural network. *Veh. Syst. Dyn.* **2019**, *59*, 396–414. [CrossRef]

22. Russell, S.J.; Norvig, P. Learning. In *Artificial Intelligence: A Modern Approach*, 3rd ed.; Pearson Education: Upper Saddle River, NJ, USA, 2010; pp. 706–868.
23. Aalizadeh, B. Comparison of neural network and neurofuzzy identification of vehicle handling under uncertainties. *Trans. Inst. Meas. Control.* **2019**, *41*, 4230–4239. [[CrossRef](#)]
24. Rajamani, R. Lateral vehicle dynamics. In *Vehicle Dynamics and Control*, 2nd ed.; Ling, F.F., Ed.; Springer: New York, NY, USA, 2006; pp. 15–48.
25. Pi, D.W.; Chen, N.; Wang, J.X.; Zhang, B.J. Design and evaluation of sideslip angle observer for vehicle stability control. *Int. J. Automot. Technol.* **2011**, *12*, 391–399. [[CrossRef](#)]
26. Pacejka, H.B. *Tire and Vehicle Dynamics*, 3rd ed.; Butterworth-Heinemann: Oxford, UK, 2012.
27. Cheng, S.; Li, L.; Yan, B.; Liu, C.; Wang, X.; Fang, J. Simultaneous estimation of tire side-slip angle and lateral tire force for vehicle lateral stability control. *Mech. Syst. Signal Process.* **2019**, *132*, 168–182. [[CrossRef](#)]
28. Singh, K.B.; Ali, A.M.; Taheri, S. An Intelligent Tire Based Tire-Road Friction Estimation Technique and Adaptive Wheel Slip Controller for Antilock Brake System. *J. Dyn. Syst. Meas. Control.* **2013**, *135*, 031002. [[CrossRef](#)]
29. Hashemi, E.; Pirani, M.; Khajepour, A.; Kasaiezadeh, A.; Chen, S.-K.; Litkouhi, B. Corner-based estimation of tire forces and vehicle velocities robust to road conditions. *Control. Eng. Pract.* **2017**, *61*, 28–40. [[CrossRef](#)]
30. Kanghyun, N.; Fujimoto, H.; Hori, Y. Lateral Stability Control of In-Wheel-Motor-Driven Electric Vehicles Based on Sideslip Angle Estimation Using Lateral Tire Force Sensors. *IEEE Trans. Veh. Technol.* **2012**, *61*, 1972–1985. [[CrossRef](#)]
31. Kunsoo, H.J.K.; Kyongsu, Y.; Dong-Il, D.C. Monitoring system design for estimating the lateral tire force. In Proceedings of the 2002 American Control Conference (IEEE Cat. No.CH37301), Anchorage, AK, USA, 8–10 May 2002; Volume 2, pp. 875–880. [[CrossRef](#)]
32. Lian, Y.F.; Zhao, Y.; Hu, L.L.; Tian, Y.T. Cornering stiffness and sideslip angle estimation based on simplified lateral dynamic models for four-in-wheel-motor-driven electric vehicles with lateral tire force information. *Int. J. Automot. Technol.* **2015**, *16*, 669–683. [[CrossRef](#)]
33. Liu, J.; Zhang, L.; Wang, Z. A Time-delay Neural Network of Sideslip Angle Estimation for In-wheel Motor Drive Electric Vehicles. In Proceedings of the IEEE 91st Vehicular Technology Conference (VTC2020-Spring), Antwerp, Belgium, 25–28 May 2020.
34. Liu, W.; He, H.; Sun, F. Vehicle state estimation based on Minimum Model Error criterion combining with Extended Kalman Filter. *J. Frankl. Inst.* **2016**, *353*, 834–856. [[CrossRef](#)]
35. Nam, K.; Fujimoto, H.; Hori, Y. Advanced Motion Control of Electric Vehicles Based on Robust Lateral Tire Force Control via Active Front Steering. *IEEE/Asme Trans. Mechatronics* **2014**, *19*, 289–299. [[CrossRef](#)]
36. Jin, X.; Yin, G. Estimation of lateral tire–road forces and sideslip angle for electric vehicles using interacting multiple model filter approach. *J. Frankl. Inst.* **2015**, *352*, 686–707. [[CrossRef](#)]
37. Jing, H.W.; Hu, C.; Wang, J.; Yan, F.; Chan, N. Vehicle lateral motion control considering network-induced delay and tire force saturation. In Proceedings of the 2016 American Control Conference, Boston, MA, USA, 6–8 July 2016.
38. Singh, K.B.; Taheri, S. Accelerometer Based Method for Tire Load and Slip Angle Estimation. *Vibration* **2019**, *2*, 174–186. [[CrossRef](#)]
39. Wei, W.; Shaoyi, B.; Lanchun, Z.; Kai, Z.; Yongzhi, W.; Weixing, H. Vehicle Sideslip Angle Estimation Based on General Regression Neural Network. *Math. Probl. Eng.* **2016**, *2016*, 3107910. [[CrossRef](#)]
40. Zhang, Z.; Chu, L.; Zhang, J.; Guo, C.; Li, J. Design of Vehicle Stability Controller Based on Fuzzy Radial Basis Neural Network Sliding Mode Theory with Sideslip Angle Estimation. *Appl. Sci.* **2021**, *11*, 1231. [[CrossRef](#)]
41. Niskanen, A.; Tuononen, A. Three Three-Axis IEPE Accelerometers on the Inner Liner of a Tire for Finding the Tire-Road Friction Potential Indicators. *Sensors* **2015**, *14*, 51–63. [[CrossRef](#)]
42. Park, H.; Gerdes, J.C. Analysis of Feasible Tire Force Regions for Optimal Tire Force Allocation with Limited Actuation. *IEEE Intell. Transp. Syst. Mag.* **2017**, *9*, 75–87. [[CrossRef](#)]
43. Singh, K.B.; Arat, M.A.; Taheri, S. Literature review and fundamental approaches for vehicle and tire state estimation. *Veh. Syst. Dyn.* **2018**, *57*, 1643–1665. [[CrossRef](#)]
44. Singh, K.B.; Taheri, S. Estimation of tire–road friction coefficient and its application in chassis control systems. *Syst. Sci. Control. Eng.* **2014**, *3*, 39–61. [[CrossRef](#)]
45. Kanghyun, N.; Sehoon, O.; Hiroshi, F.; Yoichi, H. Estimation of Sideslip and Roll Angles of Electric Vehicles Using Lateral Tire Force Sensors Through RLS and Kalman Filter Approaches. *IEEE Trans. Ind. Electron.* **2013**, *60*, 988–1000.
46. Eunjae, L.; Hojin, J.; Seibum, C. Tire Lateral Force Estimation Using Kalman Filter. *Int. J. Automot. Technol.* **2018**, *19*, 669–676.
47. Acosta, M.; Kanarachos, S. Tire lateral force estimation and grip potential identification using Neural Networks, Extended Kalman Filter, and Recursive Least Squares. *Neural Comput. Appl.* **2017**, *30*, 3445–3465. [[CrossRef](#)]
48. ISO-26262-1-5:2018; Road Vehicles Functional Safety. ISO: Geneva, Switzerland, 2018.
49. Wang, H.; Xu, Z.; Do, M.T.; Zheng, J.; Cao, Z.; Xie, L. Neural-network-based robust control for steer-by-wire systems with uncertain dynamics. *Neural Comput. Appl.* **2015**, *26*, 1575–1586. [[CrossRef](#)]
50. Gao, J.; Zhang, Y.; Du, Y.; Li, Q. Optimization of the tire ice traction using combined Levenberg–Marquardt (LM) algorithm and neural network. *Journal Braz. Soc. Mech. Sci. Eng.* **2019**, *41*, 40. [[CrossRef](#)]
51. de Jesús Rubio, J. Stability Analysis of the Modified Levenberg–Marquardt Algorithm for the Artificial Neural Network Training. *IEEE Trans. Neural Net. Learn. Syst.* **2021**, *8*, 3510–3524. [[CrossRef](#)]

-
52. Kermani, B.G.; Schiffman, S.S.; Nagle, H.T. Performance of the Levenberg–Marquardt neural network training method in electronic nose applications. *Sens. Actuators* **2005**, *110*, 13–22. [[CrossRef](#)]
 53. Rana, M.J.; Shahriar, M.S.; Shafiullah, M. Levenberg—Marquardt neural network to estimate UPFC-coordinated PSS parameters to enhance power system stability. *Neural Comput. Appl.* **2019**, *31*, 1237–1248. [[CrossRef](#)]